Transactions of the Materials Research Society of Japan 29 [2] 533-536 (2004)

Selective Formations of Fe-Included Carbon Nanocapsules and Nanotubes by Pyrolysis of Ferrocene

N. Sano, H. Akazawa, M. Uehara, T. Kikuchi*, T. Kanki
Dept. Chemical Engineering, Himeji Institute of Technology, 2167 Shosha, Himeji, 671-2201 Japan
FAX: 81-792-67-4830, e-mail: sano@mech.eng.himeji-tech.ac.jp
*Dept. Engineering Science, Himeji Institute of Technology, 2167 Shosha, Himeji, 671-2201 Japan

Fe-contained CNCs and CNTs were separately synthesized by pyrolysis of ferrocene in pure H_2 stream in a cylindrical electrical furnace whose temperature profile was controlled at 1050 °C in its center. The CNTs and CNCs were respectively formed at 988 °C upstream zone and colder downstream zone of less than 625 °C. The CNCs contained Fe with graphitic shells. Electron diffraction analysis revealed that the core Fe was orthorhombic carbide. The typical CNCs particle sizes were in the range of 11-30nm diameters with 2-40 graphitic shells. The mean particle diameter was confirmed by specific surface area measurement.
Key words: Carbon nanotube, Nanocapsule, Ferrocene, Pyrolysis

1. INTRODUCTION

Since fullernes and carbon nanotubes (CNTs) were discovered [1], other functional nano carbon materials have been synthesized such as metal-included carbon nanocapsules (CNCs) [2-5], Bucky onions [6], carbon nanohorns [7], and carbon micro coils[8]. Especially, stable spherical nano-sized particles such as carbon onions or nano capsules are expected to show excellent solid lubrication properties as nano bearing balls. Among these spherical materials, metal included particles are attractive as one can consider the application of these particles for electromagnetic and micromachine technologies. For industrial applications, it is important to develop efficient synthesis techniques.

Several common methods are known to fabricate nanocarbons, for example (1) arc discharge [9], (2) laser ablation [10], (3) plasma-enhanced chemical vapor deposition [11], and (4) thermal pyrolysis [12]. Among these methods, pyrolysis is considered to be efficient for large scale CNTs production because continuous operation can be conducted easily. In addition to these methods, ion beam [5] and electron beam [4] can be used to produce metal-included CNCs and carbon onions. Nevertheless, efficient methods to syntheze metal-included particles are demanded to developed in order to commercialize such particles. This work found that Fe-included CNCs can be produced efficiently by pyrolysis of ferrocene in pure H_2 flow in a separated location from that where CNTs is formed.

2. EXPERIMENTAL

Figure 1 schematically shows the experimental set-up used in this study. A quartz tube (inner diameter =14 mm) was inserted in a electric furnace whose maximum temperature was controlled at 1050 °C. The temperature

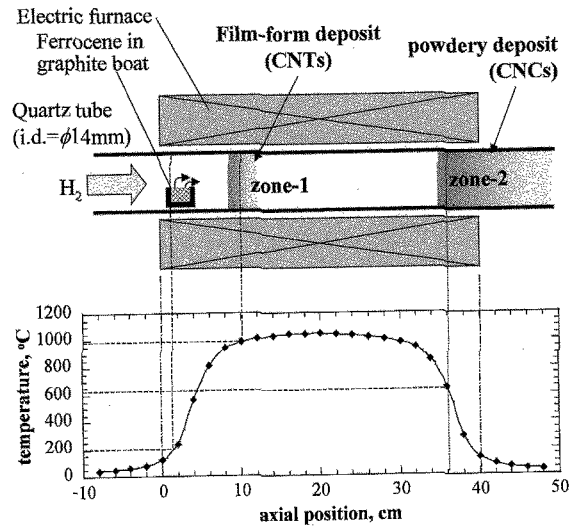

Fig. 1 Apparatus and axial temperature profile inside the electric furnace.

profile in the quartz tube is shown below the schematic. H_2 (99.99 % grade) was supplied to this reaction tube with three varied flow rates of 100, 200, 300 cm^3 min^{-1} continuously in each batch. Ferrocene Powder (88 mg) was stored in a graphite boat in the quartz tube at a upstream zone outside the furnace as initial position, and the pyrolysis was initiated by shifting the tube so that the graphite boat was transferred into the 200 °C zone. After ferrocene is transferred to the hot zone, it was sublimed and its vapor was carried to the down stream zone by H_2 gas flow. When ferrocene was pyrolized in the hot zone, solid deposits were formed in two zones, a hot zone of 988 °C (zone-1), and a relatively cool zone in downstream of less than 625°C (zone-2). The locations

of deposit zones did not depend on H_2 flow rates. After each batch of the pyrolysis was terminated, the furnace was cooled down and the resulted deposit was collected for analysis by a transmission electron microscope (TEM) attached with EDX (JEOL2010).

3. RESULTS AND DISCUSSION

3.1 Carbon nanotubes in 988 °C zone (zone-1)

The deposit which was formed in zone-1 was observed as a film-like form. Figure 2 shows a typical TEM image of this deposit. To conduct TEM observation, the deposit was ground and dispersed in toluene with sonification. It is shown that multi-walled CNTs were produced at zone-1. Under scanned TEM observation, the view similar to Fig. 2 was seen everywhere. This observation suggested that the deposit at zone-1 contains high purity MW-CNTs. One can see an important character of these MW-CNTs that they are highly winded and partially filled with a solid. EDX analysis confirmed that that the solid fillings in MW-CNTs contain Fe.

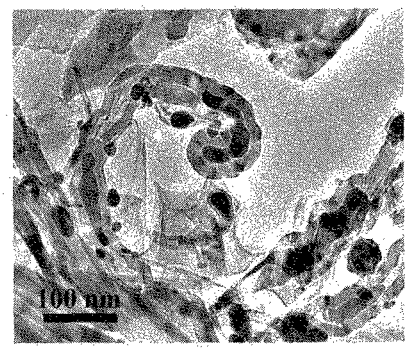

Fig. 2 TEM image of MW-CNTs formed in zone-1.

3.2 Carbon nanocapsules in 625 °C zone (zone-2)

Powdery deposits were formed in zone-2. In TEM analysis, Fe-included CNCs were found in the deposits collected from zone-2. Figure 3 shows the agglomeration of Fe-included CNCs together with a high magnification image of the marked square therein. The high magnification image shows that the Fe core was capsulated by graphite multi-layers. Scanning observation on whole sample grid area indicated that the purity of CNCs is quite high. It was interesting to notice that the concentrations of CNTs in these powders were negligible compared with the filled capsules.

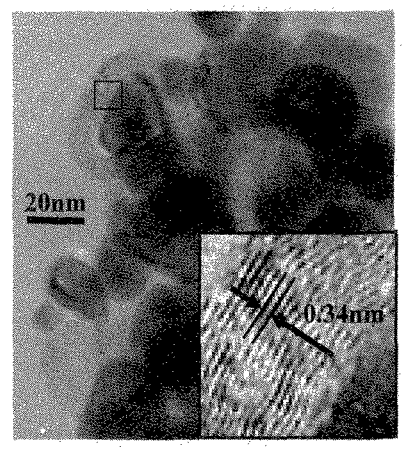

Fig. 3 TEM image of Fe-included carbon nano capsules produced in zone-2.

The filling core was considered to contain Fe from EDX analysis as shown in Fig. 4. Figure 5 shows an electron diffraction pattern taken from the core region in the CNCs. This pattern indicates that the particle core is an orthorhombic carbide Fe_3C.

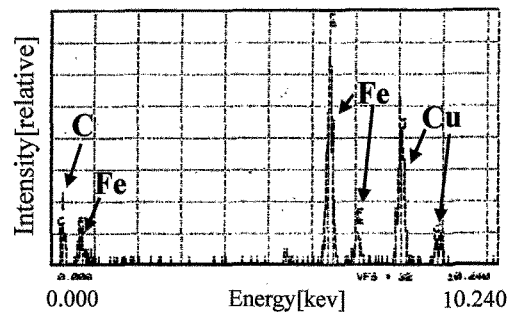

Fig. 4 EDX spectrum on cores of nano particles as shown in Fig. 3, detecting Fe. Detection of Cu is due to TE M grid.

Although most are not perfect sphere, the particles shape is considered to be nearly spherical. Figure 6 shows the statistical plot of the particle size distribution obtained from TEM observation. One can notice that 11-30 nm is the most common diameter range among whole distribution within 9 to 70 nm. The shell number was observed to range from 2 to 40 under TEM observation. In addition to TEM observation, specific surface area was measured based on BET adsorption using N_2 gas at liquid nitrogen temperature. It was resulted in 43 m^2/g. In order to evaluate mean diameter of the particle size from this value, we adopted some assumptions: (1) All particles are spherical. (2) Shell thickness is uniform. (3) The densities of the particle core and shell are uniform. From these assumptions, the approximated relationship between this specific surface

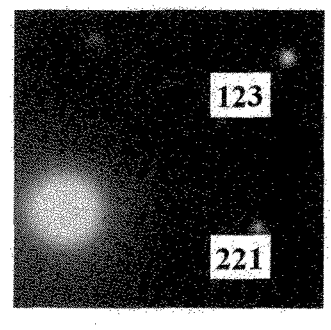

Fig. 5 Electron diffraction spots on cores of nano particles as shown in Fig. 3, indicating orthorhombic Fe_3C.

area and particle diameter is formulated by Eq. (1).

$$A = \frac{4\pi R^2}{4/3\,\pi (R_{Fe})^3 \rho_{Fe} + \{4/3\,\pi R^3 - 4/3\,\pi (R_{Fe})^3\}\rho_c} \quad (1)$$

where, A, R, R_{core}, ρ_{core}, ρ_{shell} are respectively specific surface area, particle radius, core radius, core density, and shell density. To calculate the mean particle diameter using this equation, six graphitic layer for each particle as $(R\text{-}R_{core})$=6 x 3.4nm, which was the layer number most frequently observed by TEM, and densities of the particle core and graphitic layers respectively as 7.9g/cm^3 (density of Fe) and 2.25g/cm^3 (density of graphite crystal) were adopted. As a result, the mean particle diameter is calculated as 25nm. Using the density of the observed carbide for ρ_{core}, the calculated diameter can be within 1.4 % discrepancy from this value as the density of Fe_3C is 7.72g/cm^3. In either way, the calculated result is consistent with the peak particle diameter in Fig. 6, suggesting that large size impurities are negligible in the products.

3.3 Yields of nanotubes and nanocapsules

The deposit collected from zones-1 and 2 were weighted to determine the yield. Figure 8 shows the yields of these products against H_2 gas flow rate. It is resulted that the yields of the CNTs-agglomerating film and CNCs powders are respectively around 50 % and 5 %. The yields of both products increase with H_2 flow rate gradually, but this effect is not significant. The mass of ferrocene lost during the pyrolysis, which is around 50%, was considered to be converted to gaseous byproduct. By a gas analysis using a gas chromatography suggested that CH_4 was produced as a main gas byproduct.

3.4 Formation mechanism

There are a considerable number of researches about catalytic growth of nanotubes using metallic nano particles, which are about CNTs growth by thermal pyrolysis of vapor-phase hydrocarbons [12, 14-18] and plasma-enhanced CVD method [11]. From their discussions, a plausible mechanism to form CNTs and CNCs on metallic catalyst can be summarized by carbon-solvation, diffusion in the particle or surface diffusion, and precipitation growth of graphitic structures: (1) When ferrocene is decomposed at high temperature, Fe nano particles are formed from Fe atoms emitted from ferrocene. (2) Carbonaceous precursors are decomposed at the Fe particle surface, and absorbed into the Fe nano particles. (3) Graphitic structure such as CNTs and CNCs are formed through the diffusion of carbon there. It should be noted that if carbonaceous precursors are not continuously supplied to the Fe nano particles, CNTs can not grow to a elongated structures so that spherical CNCs may be preferably formed. In the present condition, CNCs are formed separately from CNTs at the down stream region of relatively low temperature. In our survey among previous articles, such selective formation of CNCs is extremely rare. Sharon et al. reported that CNCs can be formed selectively by pyrolysis of ferrocene with camphor carried by argon [18]. Although their products are Fe-contained CNCs similar to the particles shown in this work, the diameters

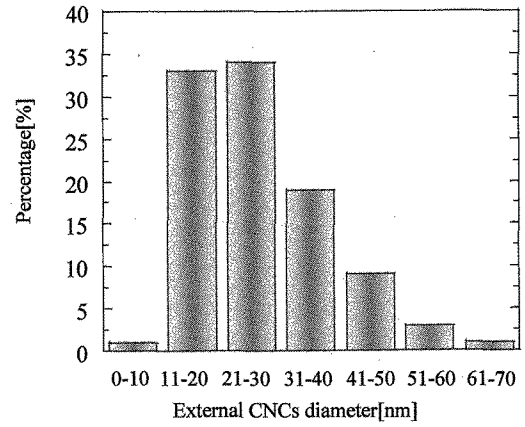

Fig. 6 Particle size distribution of Fe-included carbon nano capsules determined by TEM observations.

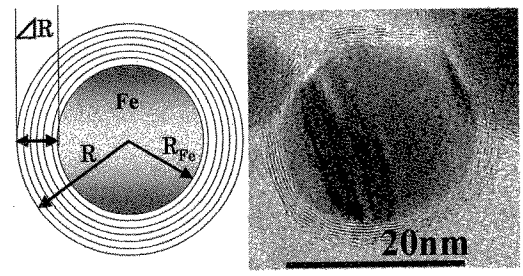

Fig. 7 Parameters used in Eq. (1).

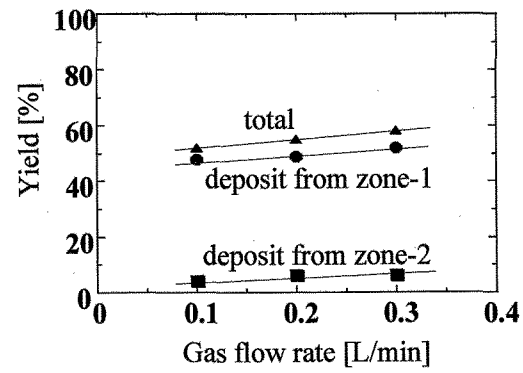

Fig. 8 Yield of Fe-CNCs (zone-2) and CNTs (zone-1) formed by pyrolysis of ferrocene in H_2 stream.

of their particles, which are about 250-850 nm, are approximately one order magnitude larger than ours. In addition, the graphitic shells of their particles are much thicker than our case. In previous reports regarding pyrolytic synthesis of carbon nano structures, carrier gas to convey evaporated ferrocene is hydrogen or inert gases mixed with hydrocarbons as carbon source. Compared with these reported experimental conditions, our condition is considered to successfully provide Fe nano-sized particles supersaturated with carbon without excessive carbonaceous precursors in the relevant region. To achieve such a condition, the use of only pure hydrogen for gas flow without admixing organic gases would be suitable, in which carbon source is only ferrocene itself.

3.5 Industrial Applications of nanocapsules

From the spherical shape of the Fe-included CNCs, it is expected that these particles show excellent tribological characteristics as solid lubricants. Tenne et al has proved that nearly spherical multi-shelled MoS_2 particles, whose diameters are typically less than 40 nm similar to our Fe-included CNCs, showed superior bribological characteristics as solid additives to lubrication oil [20], and they conclude that such characteristics are due to their spherical shape which can roll between mating surfaces just like 'nano bearing balls.' To realize this characteristics, not only the spherical shape but also the particle size is critical. In addition to such tribological properties, our Fe-included CNCs should have potential ability for some electromagnetic applications. Here it is important to notice that Fe capsulated in CNCs is protected from oxidation by stable graphite multi-shells [21] so that we can use the magnetic character of Fe nano particles very stably. Most importantly, the presented method enables ones to produce high purity Fe-included CNCs easily so that the viability of further applications should be researched within the near future.

4. CONCLUSIONS

Fe-contained CNCs and CNTs were separately formed by pyrolysis of ferrocene in pure H_2 stream through a furnace which had a temperature profile controlled at 1050 °C in its center. The Fe-included CNTs and CNCs were respectively formed at 988 °C zone and colder downstream zone of less than 625 °C. The CNCs were observed to contain Fe core. Electron diffraction analysis revealed that such Fe core is carbide. It was observed by TEM observation that the typical CNCs particle sizes were in the range of 11-30nm diameters with 2-40 graphitic shells. The mean particle diameter of CNCs estimated from a specific surface measurement was consistent with the size distribution obtained from TEM analysis. From the shape and the size of Fe-included CNCs produced by our method, they are considered to be a candidate of an excellent solid lubricant for their particle size and spherical shape in addition to the magnetic applications.

5. REFERENCES

[1] S. Iijima, *Nature*, **354**, 56-8 (1991).
[2] R. S. Ruoff, D. C. Lorents, B. Chan, R. Malhotra, S. Subramoney, *Science*, **259**, 346-7 (1993).
[3] T. Hihara, H. Onodera, K. Sumiyama, K. Suzuki, A. Kasuya, Y. Nishina, Y. Saito, T. Yoshikawa, M. Okuda, *Jpn. J. Appl. Phys. (part 2)*, **33**, L24-5 (1994).
[4] A. Yasuda, W. Mizutani, T. Shimizu, H. Tokumoto, N. Kawase, F. Banhart, *J. Phys. Chem. B*, **106**, 1247-51 (2002).
[5] E. Abe, S. Yamamoto, A. Miyashita, K. E. Sickafus, *J. Appl. Phys.*, **90**, 3353-58 (2001).
[6] D. Ugarte, Nature, 359, 707-9 (1992).
[7] S. Iijima, M. Yudasaka, R. Yamada, S. Bandow, K. Suenaga, F. Kokai, K. Takahashi, *Chem. Phys. Lett.*, **309**, 165-70 (1999).
[8] Motojima S, Kawaguchi M, Nozaki K, Iwanaga H. Appl Phys Lett; 1990; 56: 321-3.
[9] T. W. Ebbesen, P. M. Ajayan, *Nature*, **358**, 220-2 (1992).
[10] T. Guo, P. Nikolaev, A. G. Rinzler, D. Tomanek, D. T. Colbert, R. E. Smalley, *J. Phys. Chem.*, **99**, 10694-7 (1995).
[11] M. Chhowalla, K. B. K. Teo, C. Ducati, N. L. Rupesinghe, G. A. J. Amaratunga, A. C. Ferrari, D. Roy, J. Robertson, W. I. Milne, *J. Appl. Phys.* **90**, 5308-17 (2001).
[12] M. Endo, T. Takeuchi, S. Igarashi, K. Kobori, M. Shiraishi, H. W. Kroto, *J. Phys. Chem. Solids*, **54**, 1841-8 (1993).
[13] N. Sano, H. Akazawa, T. Kikuchi, T. Kanki *CARBON*, **41**, 2159-62 (2003).
[14] M. Endo, *Chemtech*, 568-76 (1988).
[15] M. Endo, Y. A. Kim, T. Matusita, T. Hayashi, "Carbon Filaments and Nanotubes", Kluwer Academic Publishers, Netherland, (2001) pp. 51-61.
[16] H.M.Cheng, F.Li,G. Su, H.Y.Pan, L.L.He, X.Sun, M.S.Dresselhaus, *Appl. Phys. Lett.* **72**, 3282-4 (1998).
[17] L. Ci, J. Wei, B. Wei, J. Liang, C. Xu, D. Wu, *Carbon*, **39**, 329-35 (2001).
[18] R. Marangoni, P. Serp, R. Feurer, Y. Kihn, P. Kalck, C. Vahlas, *Carbon*, **39** 443-9 (2001).
[19] M. Sharon, K. Mukhopadhyay, K. Yase, S. Iijima, Y. Ando, X. Zhao, *Carbon*, **36**, 507-11 (1998).
[20] L. Rapoport, Y. Bilik, Y. Feldman, M. Homyonfer, S. R. Cohen, R. Tenne, *Nature*, **387**, 791-3 (1997).
[21] Y. Saito, "Proc. Recent Advances in the Chemistry and Physics of Fullerenes and Related Materials", Ed. The Electrochemical Soc., Pennington, New Jersey, (1994) pp. 1419.

(Received October 9, 2003; Accepted November 20, 2003)